energies

MDPI

Article

Characterizing the Spatiotemporal Complexity of Power Outages in the U.S. Power Grid: A Reliability Assessment Perspective

Qun Yu [1], Zhiyi Zhou [1,*], Tongshuai Jin [1], Weimin Sun [2] and Jiongcheng Yan [3]

[1] College of Electrical and Automation Engineering, Shandong University of Science and Technology, Qingdao 266590, China; yuqun_70@163.com (Q.Y.); jtssdust@sdust.edu.cn (T.J.)
[2] China Electric Power Research Institute Co., Ltd., Beijing 100192, China; sunweimin07@126.com
[3] The Key Laboratory of Power System Intelligent Dispatch and Control of Ministry of Education, Shandong University, Jinan 250061, China; yanjc@mail.sdu.edu.cn
* Correspondence: zzysdust@sdust.edu.cn

Abstract

With the intensification of climate change, deepening energy transition, and increasing social vulnerability, extreme power outage events pose escalating challenges to the governance capacity of modern power systems. Existing evaluation frameworks primarily focus on engineering reliability and economic loss estimation, lacking systematic quantification of the governance complexity arising from multidimensional interacting pressures behind outage events. This creates a blind spot in both theoretical research and governance practice, hindering differentiated resilience decision-making. To address this gap, this study develops a four-dimensional evaluation framework of power outage governance complexity encompassing event attributes, external environment, internal system, and social impacts. Based on county-level outage data and multi-source auxiliary data in the United States from 2015 to 2024 and employing the XGBoost–SHAP interpretable machine learning approach, we construct the Power Outage Complexity Index (POCI) for all U.S. counties and systematically analyze its spatiotemporal evolution and core driving factors. The results show that outage governance complexity in the U.S. power grid exhibits a significant upward trend during 2015–2024, with an average annual growth rate of 1.84%. Spatially, significant positive autocorrelation is observed, and 146 high-complexity hotspot counties are identified, mainly clustered along the East and West Coasts, the Gulf Coast, and the Southwest. Driver analysis reveals that social impact and event attribute dimensions together account for nearly 90% of the variance in complexity, with cumulative outage exposure burden, outage frequency, and large-scale event ratio being the most critical drivers. Theoretically, this study extends power resilience research from an engineering-physical paradigm to a socio-technical governance paradigm and provides a reproducible methodological framework for assessing governance complexity in critical infrastructure systems. Practically, the POCI can serve as a governance diagnostic tool for the power industry and regulators, supporting resilience investment prioritization, emergency resource optimization, and differentiated governance strategy formulation. It also provides empirical evidence for safeguarding energy security in highly vulnerable communities and promoting energy resilience equity.

Keywords: Power Outage Complexity Index (POCI); reliability characterization; monitoring and metrics; institutional adaptation; spatiotemporal evolution; explainable machine learning

Check for updates

Academic Editor: Michael Negnevitsky

Received: 24 January 2026
Revised: 20 February 2026
Accepted: 27 February 2026
Published: 2 March 2026

Copyright: © 2026 by the authors. Licensee MDPI, Basel, Switzerland. This article is an open access article distributed under the terms and conditions of the Creative Commons Attribution (CC BY) license.

1. Introduction

The power system is a critical infrastructure of modern society, underpinning nearly all aspects of social functioning [1,2]. In recent years, driven by the intensification of climate change, the increasing frequency of extreme weather events, rapid transformation of the energy structure, and rising complexity of power grid systems, the operating environment of power grids has become more complex and uncertain [3]. This has led to more frequent power outage events and increased severity of their impacts, resulting not only in substantial economic losses but also in serious social security risks and public health crises [4].

Against this background, power outage research should no longer focus solely on the occurrence of events and their impacts magnitudes, but rather on outage complexity and how to address this emerging challenge [5,6]. For power grid operators, outages are not merely the direct consequences of equipment failures or natural disasters; they also entail complex management tasks—such as rapid fault localization, repair dispatch, and cross-departmental coordination—under constrained resources [7]. The unpredictability of extreme weather, spillover effects across regions, and the differentiated exposure of socially vulnerable populations further exacerbate the complexity of outage processes and their consequences [8,9]. Even when outage scales are similar, substantial differences exist across regions in terms of emergency response capacity, recovery pressure, and decision-making complexity. Therefore, there is an urgent need to develop a power outage complexity metric that integrates multidimensional influencing factors to support resource allocation, risk prioritization, and resilience investment.

Most existing power outage studies have primarily focused on individual outage events or localized regions. For example, in [10,11], the power outages triggered by the 2021 Texas winter storm were analyzed, with emphasis on the spatial extent and duration of outages, emergency preparedness, and social equity. In [12], a hazard-resistance-based spatiotemporal risk analysis framework was proposed and applied to simulate power outages caused by Hurricane Fiona in Puerto Rico in 2022. Similarly, in [13], the compound disaster risks induced by Hurricanes Ida and Laura were evaluated, with a particular focus on the multiple impacts of power outages in Louisiana. In [14], the relationship between frequent power outages and renewable energy supply was examined in Australia's Northern Territory. The study in [15] investigated the impacts of storms on power outages in New York State between 2017 and 2020 and assessed the spatial distribution of extreme weather events. In [16], power outages across 2447 U.S. counties from 2018 to 2020 were analyzed, revealing their widespread distribution and increasing frequency. Furthermore, in [17], grid vulnerability was quantitatively assessed for 3022 U.S. counties over the period 2014–2023, showing an overall upward trend in national grid vulnerability, particularly in high-vulnerability regions such as the East and West Coasts. Although these studies provide valuable data and analytical frameworks, they do not sufficiently address the complexity of power outages across regions and over extended time scales. Given the pronounced economic and social heterogeneity across different regions of the United States, the impacts and complexity of power outages also exhibit significant spatial variation. Therefore, large-scale, multi-temporal assessments of power outage complexity are necessary to examine the multidimensional factors involved and their interaction mechanisms.

In addition, many studies have focused on power grid vulnerability and outage-related inequality, examining the impacts of outages on different social groups and regions. In [18], mobile phone location data and nighttime light imagery were employed to assess power outage vulnerability in Harris County, Texas during Winter Storm Uri. In [17], a quantitative framework for grid vulnerability assessment was proposed, identifying urban form and structural distribution as key determinants of power grid vulnerability

in the United States. Household-level social vulnerability to long-duration outages was quantitatively evaluated in [19] using data from Colorado and Minnesota. In [20], a data-driven approach based on multi-source datasets was developed to quantify county-level social vulnerability indices in California and reveal their dynamic characteristics. The study in [16] analyzed the severity of power outages at the national county level in the United States, finding that states such as Arkansas, Louisiana, and Michigan face the dual burden of high outage exposure and medical vulnerability, thereby providing a basis for the geographic prioritization of resource allocation and intervention measures. In [21], a high-resolution spatial statistical method was proposed to examine socioeconomic inequalities associated with disaster-induced power outages and to reveal significant spatial heterogeneity in structural inequality. Moreover, based on New York City 311 power outage complaint data, the study in [22] investigated the effects of high temperatures and community characteristics on localized outages, highlighting the disproportionate outage burdens borne by low-income and minority communities. While these studies provide an important foundation for quantifying outage vulnerability, they primarily focus on differential impacts across social groups and regions and emphasize outage-related inequality. However, few studies have examined, from the perspective of power grid operation, the multidimensional pressures and governance challenges faced by different regions during power outage events, limiting their ability to support precise decision-making for resilience enhancement and emergency management.

In recent years, data-driven approaches have been increasingly introduced into power outage analysis, offering new opportunities for processing large-scale outage data. In [23], a Monte Carlo simulation was combined with outage modeling to predict outage duration and economic costs, thereby improving assessment accuracy. In [24], a clustering algorithm incorporating multiple influencing factors was proposed to predict outage-prone areas and outage probabilities. Deep learning ensemble methods were applied in [25] to predict extreme fault events in large-scale distribution networks, with weather conditions serving as key predictive variables. In [26], adversarial networks and Informer models were employed to balance power system data and improve the prediction accuracy of extreme outage events. In [27], the uncertainty quantification capabilities of generalized linear models and random forests were validated using hurricane-induced outage data. However, most existing studies focus on predicting outage occurrence or extreme losses, with limited attention to the explainable relationships between outage governance difficulty and its influencing factors, and a systematic framework for power outage complexity assessment remains lacking.

The limitations of existing studies underscore the need to develop a quantitative approach to power outage complexity that integrates multidimensional factors. Distinct from physical vulnerability assessments rooted in an infrastructure engineering perspective, this approach focuses on the systemic and structural pressures underlying regional outage governance, aiming to answer the core question of why outage events are difficult to manage and in which dimensions institutional arrangements must adapt, thereby identifying long-term mismatches between governance institutions and their task environments. To this end, this paper constructs a comprehensive evaluation indicator system from four dimensions—event attributes, external environment, internal system, and social impacts—and proposes the Power Outage Complexity Index (POCI). Using multi-source data from the United States, the spatiotemporal evolution and spatial clustering patterns of outage complexity are systematically analyzed. The results provide empirical support for enhancing power grid resilience, optimizing emergency response mechanisms, and improving cross-regional governance.

The main contributions of this paper are summarized as follows.

(1) A multidimensional evaluation framework and indicator system for power outage complexity are developed, and the Power Outage Complexity Index (POCI) is proposed.
(2) Based on multi-source U.S. data, an explainable machine learning approach is employed to determine indicator weights and identify key driving factors.
(3) The spatiotemporal patterns of county-level power outage complexity from 2015 to 2024 are systematically examined, with hotspot regions and long-term trends identified to support differentiated management strategies.

The remainder of this paper is organized as follows. Section 2 introduces the indicator system, the POCI construction methodology, and data sources. Section 3 presents the empirical results. Section 4 concludes the paper and discusses limitations.

2. Research Methods and Data

2.1. Research Ideas and Technical Route

This study adopts a large-scale, multi-source data-driven empirical approach to systematically quantify and analyze power outage complexity across the U.S. power grid over the past decade. The overall technical framework is illustrated in Figure 1 and consists of four main steps:

(1) Constructing a four-dimensional indicator system for power outage complexity encompassing event attributes, external environment, internal system, and social impacts.
(2) Determining the relative importance of each indicator and assigning objective weights using an explainable machine learning framework based on the XGBoost–SHAP model.
(3) Developing the Power Outage Complexity Index (POCI) to quantify county-level outage complexity.
(4) Applying spatial statistical methods to examine spatial clustering patterns and long-term trends in outage complexity, thereby providing analytical support for the formulation of differentiated governance strategies.

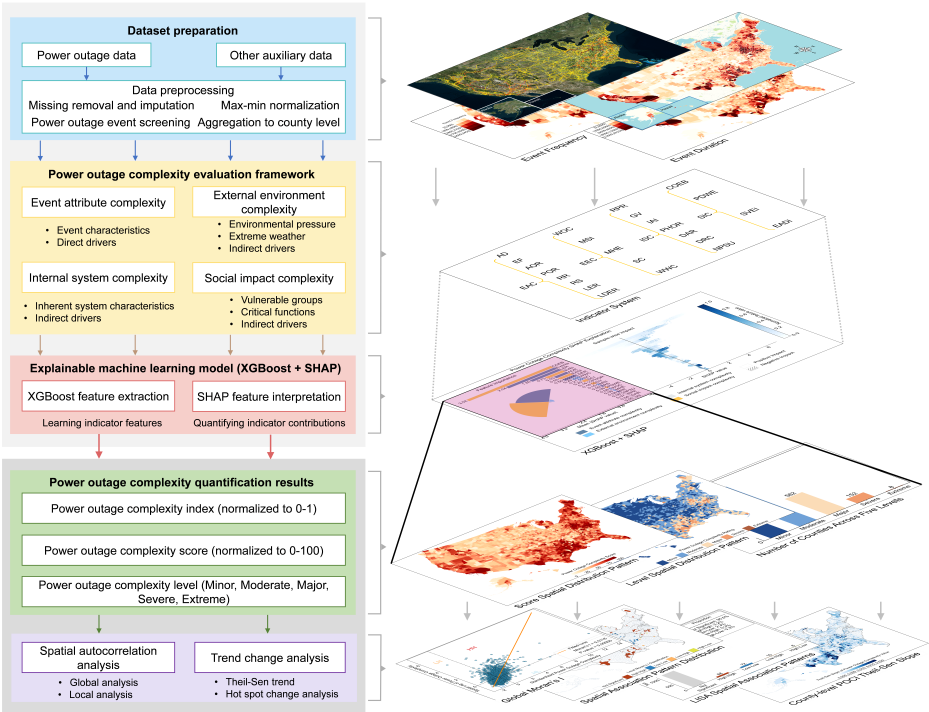


Figure 1. Technical framework for the quantification and evaluation of power outage complexity.

2.2. Construction of Power Outage Complexity Indicator System

To comprehensively quantify power outage complexity, this study proposes the Power Outage Complexity Index (POCI). The index is designed to characterize the overall pressure borne by the power governance system in responding to outage events, and its core positioning is as a systematic diagnostic tool for outage governance difficulty. Distinct from physical vulnerability assessments grounded in an infrastructure engineering perspective, POCI is intended to function as a complementary instrument that focuses on governance capacity rather than physical failure probability. Power outage complexity is reflected not only in the technical characteristics of outage events—such as scale, frequency, and duration—but also in governance-related burdens, including emergency response, resource allocation, cross-departmental coordination, and decision-making uncertainty. Accordingly, POCI captures the overall difficulty of managing power outage events under different contextual conditions. By explicitly identifying the mismatch between governance institutions and their task environments, the index provides a quantitative basis for designing differentiated governance strategies and institutional adaptation pathways.

The construction of POCI is grounded in contingency theory, which emphasizes that the effectiveness of a governance system depends on the degree of alignment between its internal structure and operational mechanisms and the complexity of the external environment [28–30]. When external conditions evolve rapidly while governance systems adjust with delay, system efficiency deteriorates substantially. In power systems, climate change, energy transition, and rising social vulnerability jointly intensify the uncertainty associated with outage governance. From this theoretical perspective, this study develops a comprehensive indicator system consisting of 22 quantitative indicators across four dimensions—event attributes, external environment, internal system, and social impacts—to systematically evaluate regional differences in power outage complexity and to provide a unified quantitative basis for cross-regional comparison and integrated resilience assessment.

Unlike vulnerability assessment frameworks constructed solely on the basis of the physical characteristics of outage events, the indicator system in this study achieves expansion along three dimensions. First, it introduces an external environment dimension to quantify the coupled stress effects between extreme weather and power outage events. Second, it adds an internal system dimension, incorporating technical characteristics such as infrastructure conditions and renewable energy penetration into the assessment. Third, it introduces a social impact dimension, endogenizing social consequences—such as social vulnerability and the intensity of economic disruption—into the index construction. Together, these extensions establish a full-chain governance complexity assessment framework structured around "pressure sources–system state–social consequences."

2.2.1. Event Attribute Complexity (EAC)

Event Attribute Complexity characterizes the fundamental properties of power outage events, including their scale, frequency, and duration. As the most direct manifestation of outage complexity, this dimension strongly influences emergency resource allocation and recovery strategy formulation. It comprises the following six indicators: (1) Event Frequency (Events): Total number of valid power outage events in a county within a year; (2) Average Outage Rate (AOR): Average proportion of customers affected by power outage events, reflecting the mean impact scale; (3) Recovery Rate (RR): Proportion of customers restored per unit time, measuring fault repair efficiency; (4) Recovery Stability (RS): Coefficient of variation of outage duration, indicating volatility in the recovery process; (5) Large-scale Event Ratio (LER): Proportion of outage affecting more than 5% of customers; (6) Long-duration Event Ratio (LDER): Proportion of events lasting longer than 8 h.

2.2.2. External Environment Complexity (EEC)

External Environment Complexity reflects the uncertainty imposed on power system operation by external disturbances such as extreme weather events. The intensity, frequency, and combined characteristics of these disturbances jointly determine the severity of the operating environment during outage occurrences. This dimension includes five indicators: (1) Weather-Outage Concurrence (WOC): Proportion of outage events occurring during extreme weather conditions; (2) Meteorological Stress Intensity (MSI): Cumulative weighted impact considering weather type, intensity, and temporal overlap; (3) Multi-hazard Exposure (MHE): Number of extreme weather types experienced by a county within a year; (4) Seasonal Concentration (SC): Degree of seasonal unevenness in outage occurrence, measured using the Gini coefficient; (5) Weather Warning Coverage (WWC): Proportion of outage events for which meteorological warnings had been issued in advance.

2.2.3. Internal System Complexity (ISC)

Internal System Complexity describes intrinsic operational characteristics of the power system, including energy structure, infrastructure condition, and system regulation capacity, which collectively determine system resilience and recovery efficiency when exposed to external disturbances. This dimension consists of seven indicators: (1) Renewable Penetration Rate (RPR): Proportion of installed wind and photovoltaic generation capacity; (2) Generation Volatility (GV): Coefficient of variation of monthly renewable energy generation; (3) Infrastructure Aging Index (IAI): Average operational age of power generation facilities; (4) Peak-hour Outage Ratio (PHOR): Proportion of outage events occurring during peak electricity demand periods; (5) Distribution Automation Rate (DAR): Proportion of customers equipped with smart meters; (6) Demand Response Capability (DCI): Ratio of load curtailment capability to its potential under emergency conditions; (7) Number of Power Supply Units (NPSU): Number of power supply entities providing distribution services within a county.

2.2.4. Social Impact Complexity (SIC)

Social Impact Complexity characterizes the comprehensive effects of power outages on social and user systems, reflecting the extent to which governance pressure spills over into societal impacts. This dimension includes four indicators: (1) Cumulative Outage Exposure Burden (COEB): Per capita power outage exposure duration at the county-year scale; (2) Population Density Weighted Exposure (PDWE): Outage impact weighted by spatial and diurnal population distribution; (3) Social Vulnerability Exposure Intensity (SVEI): Combined exposure level of social vulnerability and outage impact; (4) Economic Activity Disruption Intensity (EADI): Potential per capita economic loss intensity caused by power outages.

2.3. Construction of the Power Outage Complexity Index

To quantify power outage complexity at the U.S. county level, this study develops an explainable machine learning framework based on XGBoost and SHAP, through which the Power Outage Complexity Index (POCI), corresponding scores, and risk levels are generated [17]. XGBoost effectively captures complex nonlinear relationships via gradient-boosted decision trees, while SHAP decomposes model outputs based on Shapley values to provide feature importance and directional interpretations [31]. Compared with subjective weighting approaches, this data-driven framework ensures greater consistency and reproducibility in determining indicator weights and explicitly reveals the contributions of different factors to regional complexity differences [32].

2.3.1. Data Preprocessing

This study uses annual data for 22 indicators covering 3144 U.S. counties from 2015 to 2024. All indicators are normalized to the range [0, 1] using Min–Max scaling. For negatively oriented indicators (e.g., Recovery Rate (RR) and Distribution Automation Rate (DAR)), reverse normalization is applied to ensure consistency, such that higher values uniformly indicate higher outage complexity.

To reduce the influence of interannual variability on long-term complexity assessment and to obtain more stable county-level representations, the arithmetic mean of each indicator over the ten-year period is computed for each county and used as the training dataset.

It should be noted that the use of ten-year averages enhances statistical robustness while filtering out annual anomalies caused by single extreme events, thereby enabling POCI to focus on the structural pressures of regional outage governance; however, this treatment also smooths the instantaneous impacts of extreme events. Accordingly, POCI is positioned as a long-term structural assessment tool whose core function is to diagnose inherent pressure sources and institutional adaptation gaps in regional outage governance, rather than to evaluate emergency responses to individual events.

2.3.2. Label System Construction

A binary supervised learning strategy is adopted to learn the relative weights of the indicators. As a latent construct encompassing four dimensions—event attributes, external environment, internal system, and social impacts—power outage governance complexity cannot be directly observed or measured. Following common practices in socio-technical systems research for handling latent variables, this study employs SAIDI (System Average Interruption Duration Index) and SAIFI (System Average Interruption Frequency Index) as outcome-oriented proxy variables for governance complexity [33]. These two metrics do not directly measure outage complexity itself; rather, they reflect whether the governance system has exceeded its carrying capacity under multidimensional pressures—only when such pressures surpass the system's tolerance threshold do substantial increases in SAIDI/SAIFI become observable.

Specifically, normalized SAIDI and SAIFI values are combined into a composite reliability pressure score. Counties are then classified into low-pressure (label = 0) and high-pressure (label = 1) groups using the sample median as the threshold. Using the median as the cutoff provides a data-driven and neutral benchmark in the absence of predefined intervention standards, while also ensuring an approximately 1:1 class balance, thereby reducing the potential impact of class imbalance on model training and feature importance estimation. In addition, the 40th and 60th percentiles are employed to test the robustness of the threshold selection, with detailed results reported in Appendix C. It should be emphasized that the core objective of model training is to learn each feature's explanatory power with respect to whether the governance system exceeds its carrying threshold, rather than to directly predict SAIDI/SAIFI themselves.

2.3.3. Multicollinearity Diagnosis and Treatment

To prevent model instability and distorted SHAP interpretations caused by multicollinearity, Variance Inflation Factor (VIF) analysis is conducted prior to model training, with a threshold set at VIF = 5 [34]. An iterative elimination procedure is applied, whereby the feature with the highest VIF is removed at each step until all remaining features satisfy the threshold criterion. This process reduces collinearity risk while preserving as much information as possible.

2.3.4. XGBoost Model Training and Optimization

XGBoost is selected as the core classification model based on a comprehensive consideration of the research objectives, data characteristics, and model suitability. First, the study aims not only to achieve high predictive performance but also to objectively identify key driving factors; as a gradient boosting tree ensemble model, XGBoost effectively satisfies the dual requirements of "driver identification + index construction." Second, significant nonlinear relationships and higher-order interaction effects exist among the 22 indicators, and XGBoost can automatically capture such complex patterns without requiring pre-specified functional forms. Third, XGBoost incorporates built-in regularization mechanisms that effectively control model complexity and mitigate overfitting risk, while maintaining strong compatibility with the SHAP framework [35], thereby providing rigorous mathematical support for feature attribution and weight construction.

To address potential mild class imbalance in the training dataset, a hybrid resampling strategy combining SMOTE and Tomek Links is employed. By synthesizing minority-class samples and removing overlapping samples near class boundaries, this approach refines the decision boundary structure and enhances the model's ability to identify high governance-complexity samples as well as its overall training stability.

Model hyperparameters—including tree depth, learning rate, number of trees, and regularization coefficients—are optimized using random search combined with 10-fold cross-validation, with the F1 score as the optimization objective. The dataset is split into training and testing sets at an 8:2 ratio, and model performance is evaluated using accuracy, precision, recall, F1 score, and AUC–ROC.

2.3.5. SHAP Weight Extraction and Directional Adjustment

After model training, SHAP is used to interpret feature contributions. Based on deviations of individual predictions from the baseline, SHAP fairly allocates the marginal contribution of each input feature, with SHAP values representing feature-level contributions to model output [36].

The global influence strength of each indicator is measured by the mean absolute SHAP value across test samples and normalized to obtain final weights:

$$\omega_k = \frac{S_k}{\sum_{k=1}^{n} S_k} \tag{1}$$

where S_k denotes the mean absolute SHAP value of the k-th indicator, and ω_k represents its weight. To ensure consistency between weight direction and physical interpretation, the correlation between original feature values and their SHAP values is examined. A positive correlation indicates a positive indicator, while a negative correlation indicates a negative indicator, thereby enhancing the stability and interpretability of the weighting scheme.

2.3.6. Power Outage Complexity Index Calculation and Risk Classification

Using the SHAP-derived weights and directional information, the Power Outage Complexity Index (POCI) is constructed as a weighted sum of normalized indicators:

$$\mathrm{POCI} = \sum_{k=1}^{n} \omega_k f_k \tag{2}$$

where f_k is the normalized value of the k-th indicator.

Annual POCI values and their ten-year averages are calculated for each county. For cross-regional comparability, POCI values are transformed into a 0–100 score using percentile mapping. Subsequently, K-means clustering is applied to the ten-year average POCI for classification, and its suitability is grounded in two considerations: first, the

clustering input is a standardized and weighted one-dimensional continuous POCI, under which the spherical cluster assumption in high-dimensional space degenerates into the identification of natural break intervals in a one-dimensional setting, making it well suited for single-variable grading; second, it produces clearly defined category boundaries that facilitate policy communication and differentiated governance decision-making. Counties are ultimately classified into five outage governance complexity levels—minor, moderate, major, severe, and extreme—thereby establishing a standardized county-level risk grading framework.

2.4. Spatiotemporal Analysis Methods

2.4.1. Theil-Sen Trend Estimation

The Theil–Sen nonparametric regression method is employed to estimate the temporal trend slope of POCI. By calculating the median slope across all data point pairs, this method is robust to outliers and well suited for long-term time series containing extreme values [37]. The slope is computed as:

$$\beta = median\left(\frac{POCI_j - POCI_i}{j-i}\right), \ \forall i < j \tag{3}$$

where β denotes the trend slope; positive values indicate increasing outage complexity, while negative values indicate decreasing complexity.

2.4.2. Spatial Analysis

Global and local spatial autocorrelation statistics—Global Moran's I and Local Moran's I (LISA)—are applied to examine whether the spatial distribution of outage complexity deviates from randomness, identify spatial clustering patterns of high- and low-complexity regions, and provide spatial evidence for differentiated governance strategies.

Global Moran's I assesses nationwide spatial dependence of outage complexity [38] and is defined as:

$$I = \frac{n}{S_0} \cdot \frac{\sum_{i=1}^{n}\sum_{j=1}^{n}\omega_{ij}(x_i - \overline{x})(x_j - \overline{x})}{\sum_{i=1}^{n}(x_i - \overline{x})^2} \tag{4}$$

where ω_{ij} is the spatial weight between counties i and j; x_i and x_j denote county-level POCI values; $\overline{x}$ is the national mean; n is the number of counties; and $S_0 = \sum_{i=1}^{n}\sum_{j=1}^{n}\omega_{ij}$.

Moran's I ranges from -1 to 1, with positive values indicating positive spatial autocorrelation, negative values indicating negative spatial autocorrelation, and values near zero indicating random spatial patterns.

Local Moran's I (LISA) reveals local-scale spatial heterogeneity and identifies clustering patterns of high- and low-complexity regions [38]:

$$I_i = \frac{x_i - \overline{x}}{\sigma^2}\sum_{j=1}^{n}\omega_{ij}(x_j - \overline{x}) \tag{5}$$

where σ^2 denotes the variance of POCI.

Based on LISA results, counties are classified into four spatial types: high–high (HH) and low–low (LL) clusters, representing aggregations of high- and low-complexity counties, respectively, as well as high–low (HL) and low–high (LH) patterns, indicating spatial outliers. HH regions typically represent outage complexity hotspots, whereas LL regions correspond to relatively low-pressure areas.

2.5. Data Sources

2.5.1. Power Outage Data

Power outage data were obtained from the EAGLE-I™ platform developed by Oak Ridge National Laboratory (ORNL) [39]. The dataset has a temporal resolution of 15 min and covers the 48 contiguous U.S. states, the District of Columbia, Alaska, and Hawaii, representing approximately 92% of electricity customers nationwide.

To ensure annual consistency, outage records from January 2015 to December 2024 were selected as the study period. To exclude transient disturbances and localized fluctuations, outage events with an outage rate of no less than 0.1%—corresponding to the 60th percentile of county-level outage rates nationwide—and with relatively long durations were defined as effective outage events [16]. This threshold helps focus on outages with substantive impacts while reducing noise in the analysis.

2.5.2. Auxiliary Data

(1) County-level administrative boundary data were obtained from the TIGER/Line Shapefiles released by the U.S. Census Bureau and were used to construct spatial weight matrices for spatial analysis [40,41].
(2) Power system regional classification data were sourced from the U.S. Energy Information Administration (EIA). These data capture differences in power dispatch and market structures. The U.S. power system is divided into six major reliability regions, which are further subdivided into 25 subregions [42].
(3) Extreme weather data were collected from the National Centers for Environmental Information (NCEI) [43] and the Iowa Environmental Mesonet (IEM) [44]. This study considers 24 categories of meteorological events—including hurricanes and ice storms—that have been shown to exert significant impacts on power outages.
(4) Social vulnerability data were obtained from the Centers for Disease Control and Prevention (CDC) and the Agency for Toxic Substances and Disease Registry (ATSDR) [45]. These data are used to assess regional social capacity and resilience under disaster scenarios and public service disruptions.
(5) Energy system data were derived from EIA annual reports, including Form EIA-860 [46], Form EIA-861 [47], and Form EIA-923 [48], providing information on renewable energy installed capacity, electricity generation, and smart meter deployment.

3. Empirical Findings

3.1. Power Outage Complexity Analysis Based on Explainable Machine Learning

3.1.1. Computation of the Power Outage Complexity Index

Using the period 2015–2024 as the study window, a total of 3,536,833 power outage events were identified across the United States, with an aggregate outage duration of approximately 9.45 million hours and a cumulative impact on 1.865 billion customer interruptions. The average duration of a single outage event was 2.67 h, affecting approximately 527 customers on average.

From a temporal perspective, the number of outage events increased by 61.4% over the study period, while total outage duration rose by 132.6%, and the number of affected customers increased by 48.1%. Spatially, outage events exhibit pronounced geographic imbalance, with both frequency and impact severity significantly higher in eastern regions than in the Midwest. These patterns indicate that power outages in the U.S. grid over the past decade have become more frequent, more severe, and increasingly heterogeneous across regions, posing substantial challenges for outage management. Consequently, systematic quantitative analysis is urgently required to clarify spatial disparities and spa-

tiotemporal evolution patterns of outage events and to provide a scientific basis for targeted prevention and mitigation strategies.

Based on the 22 power outage complexity indicators, an XGBoost classification model was constructed to learn the relative importance of individual features. Following multicollinearity diagnostics, all indicators were found to have Variance Inflation Factor (VIF) values below 5, indicating no significant redundancy among features; therefore, all variables were retained. The model was trained using county-level ten-year average indicators as inputs, together with auxiliary supervisory labels, and hyperparameters were optimized through random search combined with 10-fold cross-validation (the optimal hyperparameter configuration is provided in Appendix E). The classification performance was robust, achieving an F1 score of 0.9539, accuracy of 0.9539, precision of 0.9524, recall of 0.9554, and an AUC–ROC of 0.9933 (Figure 2g), outperforming three benchmark models—Random Forest, Support Vector Machine, and AdaBoost (the complete performance comparison table for all models is provided in Appendix B). In addition, comparative experiments with and without the SMOTE + Tomek Links resampling strategy (full performance metrics are reported in Appendix D) show that the ranking of core features and the four-dimensional weight structure remain highly consistent, indicating that the resampling strategy does not introduce systematic bias into the SHAP interpretation results and that the weight structure of POCI is both robust and unbiased.

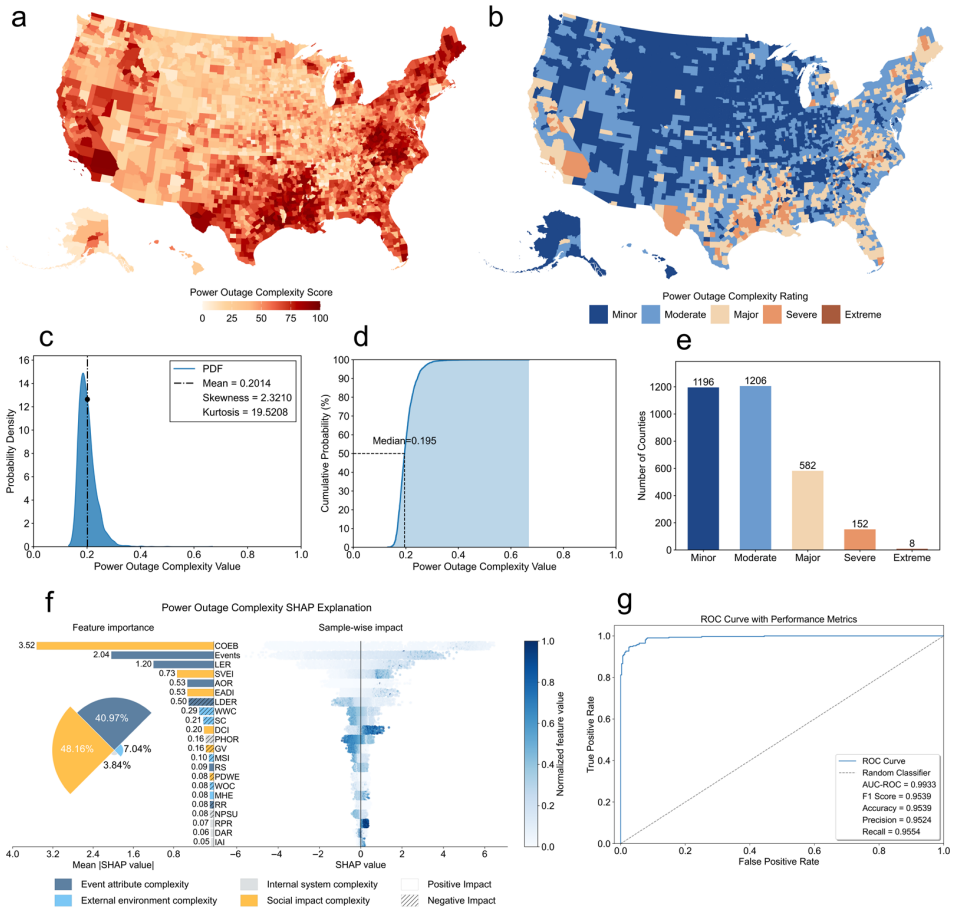


Figure 2. Statistical summary of power outage complexity in the U.S. power grid (2015–2024): (**a**) Spatial distribution of county-level power outage complexity scores; (**b**) Spatial distribution of county-level power outage complexity levels; (**c**) Probability density function (PDF) of the Power Outage Complexity Index (POCI); (**d**) Cumulative distribution function (CDF) of the Power Outage Complexity Index (POCI); (**e**) Number of counties across five power outage complexity levels; (**f**) Importance distribution of the 22 feature indicators and the four complexity dimensions; (**g**) AUC–ROC curve and performance metrics of the XGBoost model.

Feature importance was quantified using SHAP values (Figure 2f). The results show that Cumulative Outage Exposure Burden (COEB), Event Frequency (Events), and Large-scale Event Ratio (LER) rank as the top three contributors, with a combined importance of 62.23%. Table 1 summarizes the directional contributions of the major indicators. From a dimensional perspective, the social impact dimension (44.85%) and the event attribute dimension (40.96%) jointly account for 89.21% of total importance, whereas the external environment and internal system dimensions together contribute only 10.80% (Figure 2f).

Table 1. Directional contributions of major indicators to power outage complexity (SHAP).

Indicator Category	Indicators (Abbreviations)
Positive contribution (higher value indicates higher complexity)	COEB, Events, WWC, SC, GV, RS, PDWE, RR, NPSU, RPR
Negative contribution (higher value indicates lower complexity)	LER, SVEI, AOR, LDER, EADI, DCI, PHOR, MSI, MHE, WOC, DAR, IAI

These findings indicate that power outage complexity is primarily driven by exposure burden and event intensity. Specifically, COEB, Events, LER, SVEI, AOR, EADI, and LDER emerge as the core drivers of complexity variation. This pattern suggests that in mature power systems such as the United States, where baseline physical reliability has largely been established and routine faults are addressed through standardized engineering procedures, the marginal contribution of conventional infrastructure factors to governance complexity is relatively limited; instead, governance pressure is predominantly shaped by the coupling between event shock intensity and social impact amplification.

The relatively low contribution of the internal system dimension can be attributed to generally small SHAP importance values for most indicators within this dimension, with several exhibiting negative contributions. This does not negate the importance of infrastructure; rather, it indicates that internal system conditions function more as foundational constraints of governance capacity than as primary differentiating factors—once event intensity and social impact are accounted for, inter-county variations in internal system characteristics exhibit limited marginal discriminative power in explaining governance complexity. It should also be noted that this statistical pattern may reflect both the structural characteristics of mature power grids and the specific institutional context of the United States; in developing regions where infrastructure disparities remain pronounced, internal system variables may play a substantially more prominent role in shaping governance complexity.

Accordingly, inter-county differences in outage complexity are not primarily explained by variations in grid infrastructure alone but are more strongly driven by the exposure and uneven impacts of outage consequences, as well as the governance burden associated with large-scale events. Governance assessment should therefore shift from a narrow focus on grid reliability toward a more integrated consideration of social consequences, emergency response capacity, and resource coordination.

3.1.2. Spatiotemporal Distribution of Power Outage Complexity

Using SHAP-derived weights, county-level Power Outage Complexity Index (POCI) values were calculated. The complexity scores were mapped to a [0, 100] range using percentile transformation, and K-means clustering was applied to classify counties into five complexity levels.

From a statistical distribution perspective, the probability density curve of POCI values (Figure 2c) exhibits a pronounced peak at low values and a clear long right tail. The cumulative distribution function (Figure 2d) rises rapidly in the low-value range and

gradually flattens at medium-to-high values, forming a typical "sharp peak–heavy tail" and strongly right-skewed distribution. This pattern indicates that while most counties experience relatively low outage complexity, a small number of high-complexity counties substantially widen the overall distribution, producing a "many low–few high" structural imbalance. Statistically, this phenomenon is consistent with the heavy-tailed characteristics of outage impacts reported in previous studies [49,50], suggesting that outage governance pressure is highly uneven and concentrated, and that priority should be given to key regions in resource allocation.

Spatially, the distribution of POCI values (Figure 2a) reveals pronounced spatial heterogeneity and regional clustering across the United States. High-complexity regions are primarily concentrated in:

(1) the eastern coastal areas, including the Northeast metropolitan corridor, the Appalachian region, and Florida;
(2) the Gulf Coast, including Louisiana, Texas, Mississippi, and Arkansas;
(3) the Great Lakes region, particularly Michigan;
(4) the western coastal region, such as California and Idaho.

These regions are typically subject to multiple overlapping pressures, including frequent extreme weather events, dense populations and economic activity, aging infrastructure, and elevated social vulnerability, resulting in higher outage complexity. In contrast, Alaska and Hawaii exhibit relatively low complexity levels, potentially due to differences in outage scale, population density, and statistical reporting practices.

In terms of complexity class distribution, among the 3144 counties analyzed, the "minor" and "moderate" categories account for the largest shares, at 38.04% and 38.35%, respectively. The "major," "severe," and "extreme" categories together comprise approximately 23.60% of counties, of which 160 counties fall into the "severe + extreme" categories, representing 5.09% of the total and constituting priority areas for governance intervention (Figure 2e). High-complexity counties are mainly clustered in eastern coastal metropolitan areas, the Gulf Coast, and the West Coast (Figure 2b), consistent with the spatial patterns described above.

Specifically, the eight counties classified as "extreme" complexity are Tensas Parish, Louisiana [51,52]; Alamance County, Durham County [53], Henderson County [54], Mecklenburg County, New Hanover County [55], and Vance County in North Carolina; and Waynesboro City, Virginia. These counties and cities are predominantly located in developed metropolitan regions with dense populations and are subject to compounded challenges including infrastructure aging, extreme weather exposure, social vulnerability, and natural hazards, leading to the highest levels of power outage complexity.

3.1.3. Operator-Level (ISO/RTO) Analysis

To further identify structural differences in power outage complexity across the electricity operation system, county-level outage complexity scores and classifications were aggregated to the ISO/RTO level under the North American Electric Reliability Corporation (NERC). The analysis covers 25 operating regions in the contiguous United States, as well as Alaska and Hawaii, resulting in 27 analytical units.

The results (Figure 3a) indicate pronounced disparities in outage complexity across operating regions. CASO (81.06) and MISS (72.19) exhibit average complexity scores exceeding 70. In addition, FRCC (67.16), NYUP (66.74), SRCA (64.76), TRE (64.62), PJMD (64.47), CANO (62.43), PJME (60.84), and SPPS (60.62) all report average scores above 60. These high-complexity regions are predominantly located along the eastern coastline, the southern United States, and California, indicating that these areas face particularly elevated and multidimensional pressures in power outage governance.

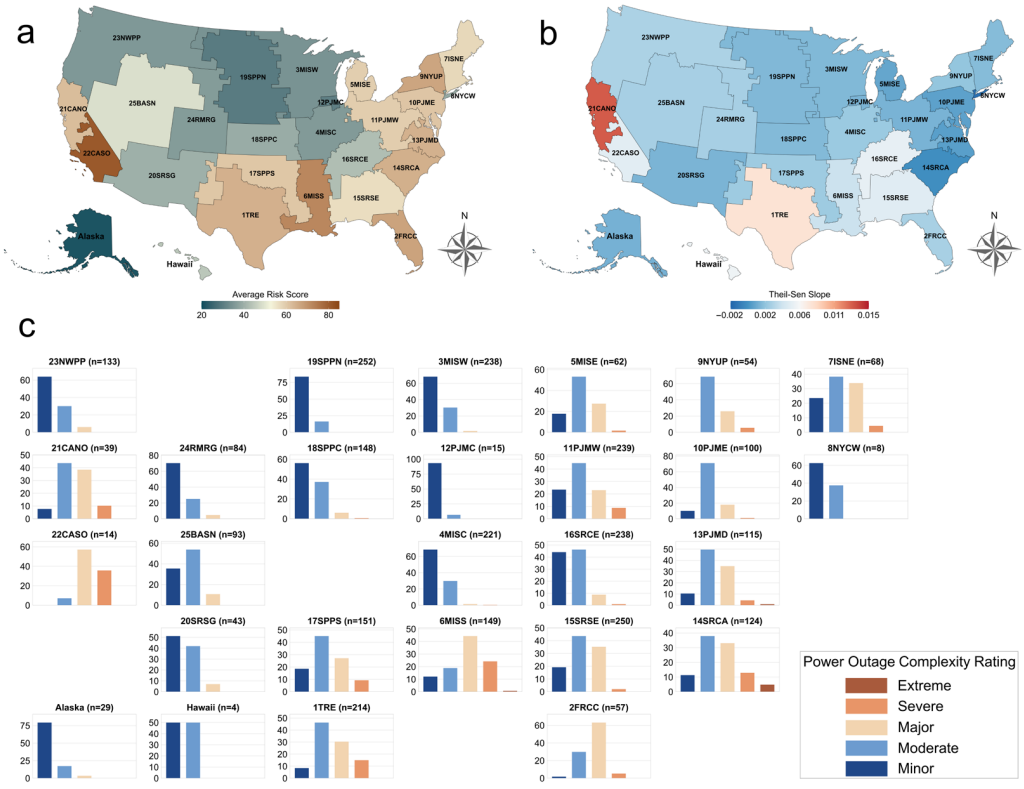


Figure 3. Spatial distribution of power outage complexity in the U.S. power grid at the ISO/RTO level: (**a**) Spatial distribution of power outage complexity scores across power system operators; (**b**) Spatial distribution of Theil–Sen slope trends of power outage complexity indices across operators; (**c**) Spatial distribution of power outage complexity levels across power system operators.

Based on time series of the Power Outage Complexity Index (POCI) for each operating region from 2015 to 2024, the Theil–Sen robust regression method was applied to estimate long-term trends (Figure 3b). The results show that outage complexity increased in 25 regions (Theil–Sen slope > 0.0001). Among them, CANO exhibits the fastest growth rate (slope = 0.0130), followed by TRE (0.0080), Hawaii (0.0060), SRCE (0.0056), CASO (0.0053), and SRSE (0.0052). Only NYCW (−0.0015) and SRCA (−0.0001) display slight declining trends. Overall, U.S. power system operators have generally experienced sustained growth in outage complexity over the past decade. The situation is particularly severe in California (CANO and CASO); Texas (TRE) has consistently maintained high complexity levels due to its independently operated grid; outage complexity in the southeastern regions has increased rapidly, likely associated with frequent hurricane impacts; and although PJM subregions exhibit slower growth rates, their absolute complexity levels remain relatively high, indicating a plateauing but persistently elevated governance burden.

Further analysis of the complexity class composition across operating regions (Figure 3c) shows that nearly all regions contain counties classified as “moderate” complexity or higher. Specifically, 23 regions include counties in the “major/severe/extreme” categories, and 17 regions contain “severe/extreme” counties. Only three operating regions include counties classified as “extreme” complexity: RCA (6 counties), MISS (1 county), and PJMD (1 county). Notably, NYUP and CASO contain no counties classified as “minor” complexity, with all counties falling into the “moderate” or higher categories.

In terms of the proportion of counties by complexity level, the three regions with the highest shares of “major/severe/extreme” counties are CASO (92.85%), MISS (69.13%), and FRCC (68.42%). Similarly, the regions with the highest proportions of “severe/extreme” counties are CASO (35.71%), MISS (24.83%), and SRCA (17.74%).

These findings demonstrate that power outage complexity in the United States is widely distributed at the operator level, with the vast majority of operating regions already experiencing moderate or higher complexity. In several regions, governance pressure is particularly pronounced, highlighting the urgent need for targeted response strategies and differentiated resource allocation.

3.2. Spatial Autocorrelation and Pattern Clustering of Power Outage Complexity

3.2.1. Global Spatial Autocorrelation Analysis

Based on the Power Outage Complexity Index (POCI) for 3144 U.S. counties over the period 2015–2024, Global Moran's I was employed to quantify the spatial clustering characteristics of outage complexity. The results indicate a Moran's I value of 0.5116 (Z-score = 48.48, $p < 0.000001$) (Figure 4c), which is substantially higher than the values commonly reported in related studies (typically 0.2–0.45) [56,57]. This result provides strong evidence of significant positive spatial autocorrelation in county-level power outage complexity across the United States.

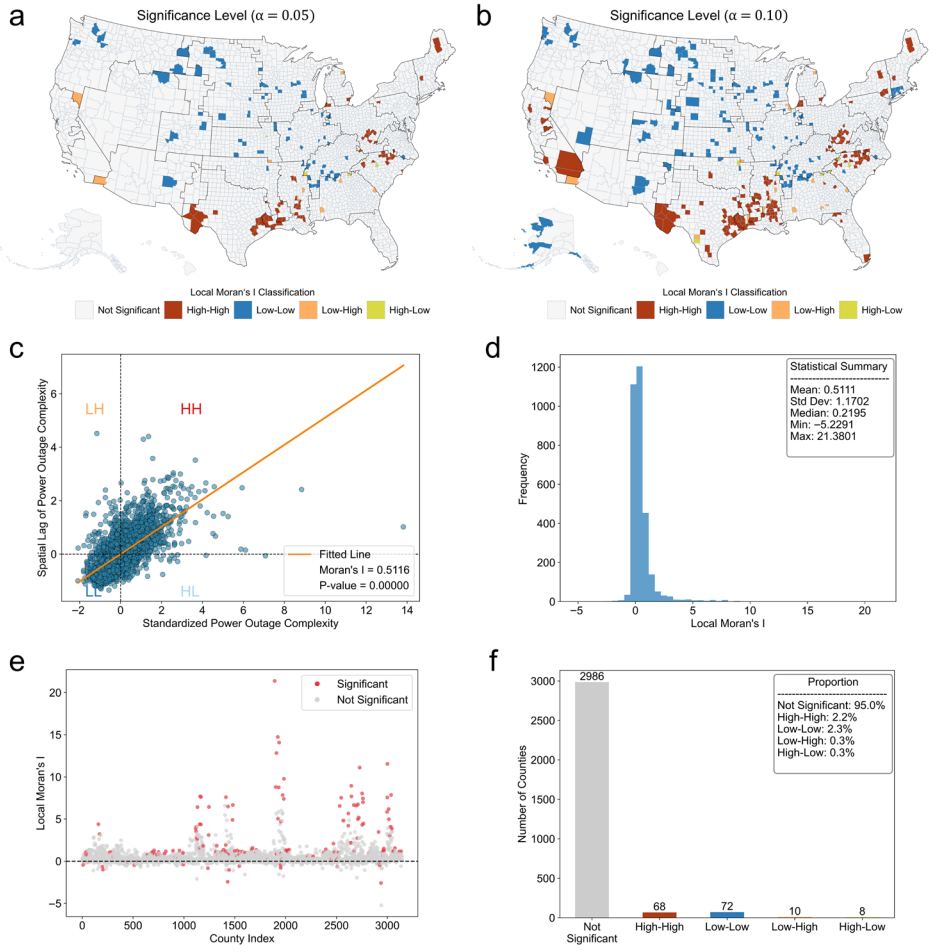


Figure 4. Spatial autocorrelation statistics, tests, and pattern distribution of county-level power outage complexity in the United States: (**a**) Distribution of five types of spatial association patterns at the significance level α = 0.05; (**b**) Distribution of five types of spatial association patterns at the significance level α = 0.10; (**c**) Global spatial autocorrelation Moran scatter plot; (**d**) Distribution of local spatial autocorrelation statistics (I_i); (**e**) Local spatial autocorrelation significance map (α = 0.05); (**f**) Proportion of LISA cluster categories (α = 0.05).

Specifically, counties with high outage complexity tend to be spatially clustered, forming contiguous high-value regions, while counties with low complexity exhibit corre-

sponding low-value clustering. The overall spatial distribution deviates markedly from randomness. These findings suggest that outage complexity is not an isolated local phenomenon but is closely associated with the operational pressures and external disturbances experienced by neighboring regions, reflecting a pronounced spatial spillover and cross-regional linkage of risk.

3.2.2. Local Spatial Autocorrelation Analysis

To further identify local-scale spatial heterogeneity in power outage complexity, Local Moran's I (LISA) was applied, and counties with statistically significant spatial associations were identified using Monte Carlo permutation tests (Figure 4d,e).

At a significance level of $\alpha = 0.05$ (Figure 4a), a total of 68 significant high–high (HH) hotspot counties (2.2%), 72 significant low–low (LL) coldspot counties (2.3%), 10 low–high (LH) outliers, and 8 high–low (HL) outliers were identified (Figure 4f). The mean complexity index of hotspot counties is 0.3194 ± 0.0570, approximately 2.10 times that of coldspot counties (0.1521 ± 0.0053). Coldspot counties exhibit relatively low internal variability, indicating a consistent level of low outage complexity. In contrast, hotspot counties show greater dispersion in complexity values, reflecting substantial intra-regional heterogeneity in governance pressure and suggesting that high-complexity areas may offer greater scope for targeted intervention. Table 2 summarizes the LISA classification results under different significance levels.

Table 2. LISA classification statistics under different significance levels.

Classification	$\alpha = 0.001$	$\alpha = 0.010$	$\alpha = 0.050$	$\alpha = 0.100$
No Significant	3139 (99.8410%)	3117 (99.1412%)	2986 (94.9745%)	2832 (90.0763%)
High-High	1 (0.0003%)	10 (0.3181%)	68 (2.1628%)	146 (4.6437%)
Low-Low	2 (0.0636%)	11 (0.3498%)	72 (2.2901%)	134 (4.2621%)
Low-High	1 (0.0318%)	4 (0.1272%)	10 (0.3181%)	20 (0.6361%)
High-Low	1 (0.0318%)	2 (0.0636%)	8 (0.2544%)	12 (0.3816%)

Spatially, significant hotspot counties are primarily concentrated in the eastern coastal region, the Gulf Coast, and the southwestern United States. Approximately 83.8% of hotspot counties are located within the MISS (27.9%), PJMW (17.6%), SRCA (19.1%), and TRE (19.1%) operating regions. These areas are commonly exposed to multiple overlapping stressors, including frequent extreme weather events (e.g., hurricanes in the MISS region, cold waves and hurricanes in TRE), aging infrastructure, and high load density.

In contrast, coldspot counties are mainly distributed across the Midwestern and north-central United States, with 87.5% of coldspots concentrated in seven operating regions. Among them, SRCE accounts for the largest share (18.1%). Coldspot regions generally face lower natural hazard risks, exhibit more stable grid operations, and benefit from higher management efficiency. Consequently, governance strategies in these regions may emphasize routine maintenance and preventive risk management.

When the significance level is relaxed to $\alpha = 0.10$ (Figure 4b), the number of hotspot counties increases to 146, and some regions that were previously not statistically significant—such as parts of PJMW and SPPS—begin to exhibit hotspot characteristics. This shift further indicates that power outage complexity in the United States demonstrates a robust spatial clustering tendency, with high-complexity patterns in certain regions becoming increasingly apparent under less restrictive statistical conditions, highlighting pronounced geographic inequality in outage complexity.

Overall, the spatial analysis reveals strong regional differentiation in power outage complexity across the United States. High-complexity areas are typically located in regions

characterized by frequent extreme climate events, dense population and economic activity, and elevated infrastructure stress, whereas low-complexity areas are more commonly found in regions with lower disaster risk and relatively stable system operation. This spatial pattern provides clear policy implications: hotspot regions should prioritize investments in disaster early warning systems, infrastructure upgrading, and grid recovery capacity, while coldspot regions may focus on routine infrastructure maintenance and preventive risk management.

3.3. Trend Analysis of Power Outage Complexity

Based on the Theil–Sen robust regression method, power outage complexity across the U.S. power grid exhibits a significant upward trend over the period 2015–2024, with an average slope of 0.00288 (t = 35.41, $p < 0.001$). The distribution of slope values is characterized by a right-skewed and sharply peaked heavy-tailed pattern (skewness = 1.58; kurtosis = 8.23) (Figure 5c), indicating that while a small number of counties experienced rapid increases in outage complexity (maximum slope = 0.044), the majority exhibited relatively moderate growth (Figure 5f). This pattern reflects pronounced heterogeneity in the evolution of outage complexity and suggests that "one-size-fits-all" approaches to grid resilience enhancement should be avoided. Instead, differentiated governance strategies are required, with priority regions focusing on disaster resilience enhancement, while other regions emphasize routine maintenance and management.

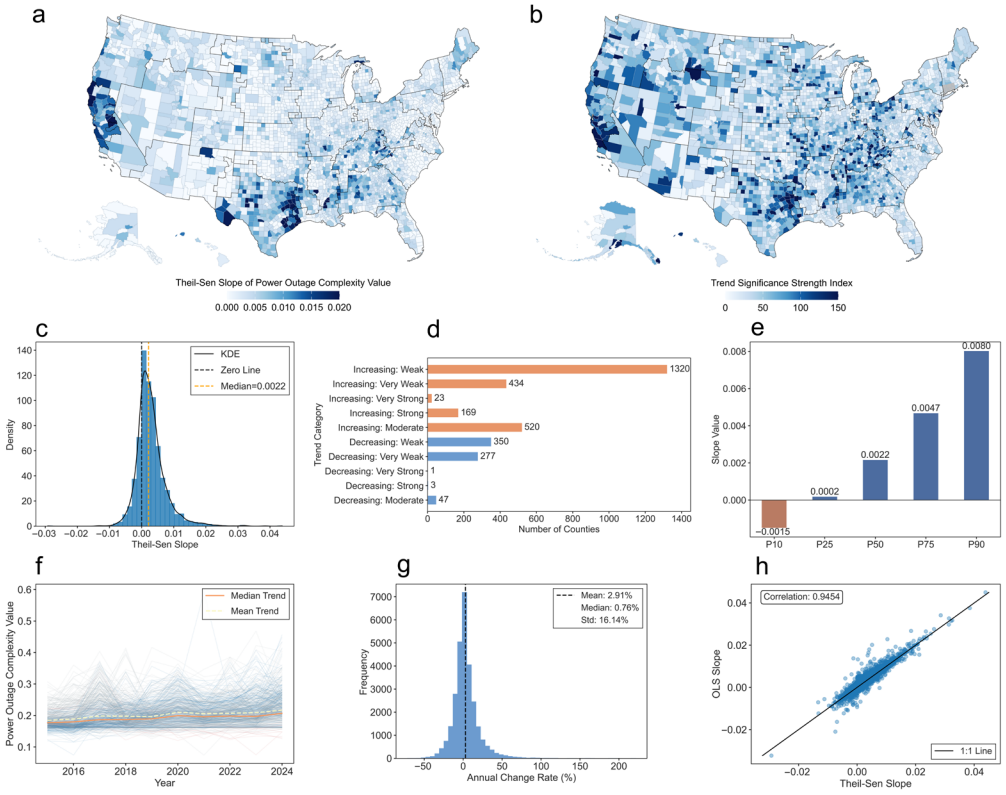


Figure 5. Trend analysis of the county-level Power Outage Complexity Index (POCI) in the United States: (**a**) Spatial distribution of Theil–Sen slopes of county-level power outage complexity (2015–2024); (**b**) Spatial distribution of Theil–Sen slope significance strength of county-level power outage complexity (2015–2024); (**c**) Histogram of Theil–Sen slope distribution; (**d**) Combined distribution of trend direction and intensity; (**e**) Bar chart of slope percentiles; (**f**) Fan chart of power outage complexity time series for 500 counties; (**g**) Histogram of annual change rate distribution; (**h**) Scatter plot comparing Theil–Sen and OLS regression slopes.

Further analysis shows that 31.6% (993 counties) experienced a significant increase in outage complexity, 65.8% (2069 counties) exhibited no significant change, and only 2.6% (82 counties) showed a decline. Counties with rapid growth are mainly concentrated along the western coast (California), the Gulf Coast (Texas, Louisiana, Mississippi, and Alabama), and parts of the eastern United States (Tennessee and Kentucky), where Theil–Sen slopes exceed 0.020 (Figure 5a). These results indicate that outage complexity in these regions has intensified markedly over the past decade, requiring grid operators to adopt more flexible resource allocation and emergency response mechanisms, particularly through targeted interventions in high-complexity areas.

To further assess the stability and reliability of trends, this study introduces the Trend Significance Strength (TSS) index, which quantifies trend robustness as the ratio of the absolute slope to the width of its confidence interval. Among 3135 valid counties, only 7.6% (237 counties) exhibit strong trends (TSS > 100), whereas 67.1% (2102 counties) have TSS values below 50, indicating that trend estimates for most counties are accompanied by substantial uncertainty (Figure 5b). Nevertheless, regions such as the western coast, Texas, and the southern Appalachian area display relatively high TSS values, suggesting that outage complexity trends in these areas are more systematic and persistent. Notably, only 0.4% (11 counties) have TSS values exceeding 200, corresponding to extremely strong trends, while 90% of counties have TSS values below 90.08. These findings highlight that reliance on slope magnitude alone may be misleading, and that combined evaluation using TSS provides a more accurate assessment of outage complexity trends, thereby offering stronger support for differentiated governance strategies.

Percentile-based analysis further confirms the widespread upward trend in outage complexity (Figure 5e), with at least 75% of counties exhibiting positive trends (Cohen's d = 0.63). High-complexity counties show particularly pronounced trend dynamics, especially those characterized by an "increasing–very strong intensity" pattern (Figure 5d). This indicates that these regions require more precise and proactive governance measures to cope with escalating outage complexity. Despite considerable fluctuations in some counties, the overall results demonstrate a systematic increase in power outage complexity across the United States over the past decade (Figure 5f), reflecting insufficient adaptability of existing grid governance systems and underscoring the urgent need for policy adjustments and strengthened emergency response mechanisms.

This study also examines the distribution of year-to-year change rates in outage complexity over the ten-year period. The mean annual change rate is 2.91%, with a median of 0.76% and a standard deviation of 16.14% (Figure 5g). The distribution is right-skewed, indicating generally moderate year-to-year changes punctuated by occasional extreme fluctuations. This pattern is consistent with the "sharp peak–heavy tail" characteristics observed in the slope distribution, suggesting that outage complexity evolution reflects both gradual accumulation and event-driven shocks. Consequently, institutional design must strike a balance between routine governance and emergency response capacity.

A comparison between Theil–Sen slopes and ordinary least squares (OLS) slopes reveals a high correlation (r = 0.945, Figure 5h), but with statistically significant differences (paired t-test: $t = 8.10$, $p < 0.001$) and a mean absolute difference of 0.00097. Given the pronounced non-normality of the data (Shapiro–Wilk W = 0.891, $p < 0.001$; Kolmogorov–Smirnov test $p < 0.001$), the Theil–Sen method demonstrates superior robustness to extreme values. In particular, it effectively suppresses outlier influence within the slope range −0.029 to 0.044, making it more suitable for time-series analyses involving multiple extreme events.

In summary, this study provides robust statistical evidence of a systematic deterioration in power outage complexity across the United States over the past decade, re-

vealing substantial spatial heterogeneity and strong statistical robustness of the observed trends. These findings offer a clear empirical basis for developing more adaptive and responsive power grid governance strategies, highlighting the urgency of institutional and policy reform.

4. Conclusions and Outlook

This study constructed a Power Outage Complexity Index (POCI) based on four dimensions—event attributes, external environment, internal system conditions, and social impacts—to quantify and analyze the multidimensional pressures faced by U.S. counties in responding to power outage events during 2015–2024. Through a data-driven approach, the spatiotemporal evolution patterns of outage governance complexity across the U.S. power grid were systematically revealed. The results indicate that outage complexity in the U.S. power system has exhibited a significant and systematic upward trend over the past decade, with pronounced spatial and temporal heterogeneity across regions. Spatial analysis identified 146 high-complexity hotspot counties, primarily concentrated along the East and West Coasts, the Gulf Coast, and the Southwestern region, suggesting clear limitations in the current state-led governance mechanisms when addressing cross-regional risks. Driver analysis further demonstrates that the social impact and event attribute dimensions together account for 89.21% of the variation in complexity, with cumulative outage exposure load, outage event frequency, and the proportion of large-scale events emerging as the most critical driving factors. These findings highlight the need to shift the governance focus from solely enhancing technical reliability toward comprehensively managing outage consequences and their associated social impacts. Overall, the results underscore the value of POCI as a diagnostic tool for evaluating outage governance difficulty in the U.S. power grid, providing a new theoretical framework and quantitative instrument to support resilience enhancement, emergency response optimization, and cross-regional collaborative governance. The index offers practical guidance for policymakers, grid operators, and emergency managers to optimize outage governance strategies under resource constraints and to strengthen overall grid resilience.

This study has certain limitations that warrant further improvement in future research. First, the supervisory training labels could be replaced with engineering-oriented labels that are more directly aligned with governance complexity, and counties located near the binary threshold could be examined through more fine-grained boundary analyses. Second, the calculation of the POCI is based on ten-year average values of the feature indicators, which may not fully capture short-term fluctuations induced by extreme events; future studies could adopt more granular temporal data slices to better reflect transient shocks. Third, alternative clustering approaches, such as Gaussian Mixture Models, may be employed to refine the classification of complexity levels.

Author Contributions: Conceptualization, Z.Z. and Q.Y.; methodology, Z.Z. and J.Y.; software, Z.Z.; validation, Z.Z., T.J. and Q.Y.; formal analysis, Z.Z. and J.Y.; investigation, Z.Z. and J.Y.; resources, W.S.; data curation, T.J.; writing—original draft preparation, Z.Z.; writing—review and editing, Q.Y. and J.Y.; visualization, Z.Z.; supervision, Q.Y.; project administration, W.S.; funding acquisition, J.Y. All authors have read and agreed to the published version of the manuscript.

Funding: This research was funded by the National Natural Science Foundation of China, grant number 52307113, and by the Science and Technology Project of State Grid Corporation of China, "Research on the Fundamental Theory of New Power System Complexity and Risk Assessment Applications", grant number 52993225000Y-034-ZN.

Data Availability Statement: The data presented in this study are available on request from the corresponding author.

Conflicts of Interest: Author Weimin Sun was employed by the company China Electric Power Research Institute Co., Ltd. The remaining authors declare that the research was conducted in the absence of any commercial or financial relationships that could be construed as a potential conflict of interest. The authors declare that this study received funding from Science and Technology Project of State Grid Corporation of China.

Appendix A

Definitions of Power Outage Complexity Indicators:

1. Event attribute complexity (EAC)

(1) Event Frequency (Events)

The total number of valid power outage events identified within a county-year unit, reflecting the frequency of outage occurrences [33].

$$\text{Events} = N_{total}$$

where N_{total} is the total number of events meeting the threshold condition (OCR $\geq$ 0.1%).

(2) Average Outage Rate (AOR)

The average proportion of customers affected across all outage events in a county-year, reflecting the average impact scale of outages [58].

$$\text{AOR} = \frac{\sum\left(\frac{C_{i,max}}{C_{i,total}}\right)}{N} \times 100\%$$

where $C_{i,max}$ is the maximum number of affected customers during event i; $C_{i,total}$ is the total number of customers served in the county.

(3) Recovery Rate (RR)

The proportion of customers restored per unit time, reflecting the fault repair efficiency of the power system [59].

$$\text{RR} = \frac{\sum\left(\frac{C_{i,max}}{D_i}\right)}{N}$$

where D_i is the duration (in hours) of event i. The unit of this indicator is customers/hour.

(4) Recovery Stability (RS)

The coefficient of variation (CV) of event durations, reflecting the predictability and volatility of outage recovery times [60].

$$\text{RS} = \frac{\sigma_D}{\mu_D}$$

where σ_D is the standard deviation of outage durations; μ_D is the mean of outage durations; CV is the coefficient of variation (dimensionless).

(5) Large-scale Event Ratio (LER)

The proportion of events affecting more than 5% of customers relative to the total number of events, reflecting the frequency of large-scale outage events [61].

$$\text{LER} = \frac{N_{large}}{N_{total}} \times 100\%$$

where N_{large} is the total number of events meeting the threshold condition (OCR $\geq$ 5%).

(6) Long-duration Event Ratio (LDER)

The proportion of events lasting longer than 8 h relative to the total number of events, reflecting the frequency of prolonged outages [16].

$$\text{LDER} = \frac{N_{long}}{N_{total}} \times 100\%$$

where N_{long} is the number of events with a duration greater than 8 h.

2. External environment complexity (EEC)

(1) Weather-Outage Concurrence (WOC)

The proportion of outage events occurring during extreme weather conditions relative to the total number of events, reflecting the direct driving effect of meteorological hazards on power outages [62].

$$\text{WOC} = \frac{N_{weather}}{N_{total}} \times 100\%$$

where $N_{weather}$ is the number of outage events spatiotemporally overlapping with recorded extreme weather. Overlap condition: an NWS-recorded extreme weather event occurred in the county during the outage event period.

(2) Meteorological Stress Intensity (MSI)

The cumulative weighted impact of extreme weather on outage events, considering weather type, intensity, and degree of temporal overlap [63].

$$\text{MSI} = \frac{\sum[\sum(I_k \times Severity_{i,k} \times Overlap_{i,k})]}{N}$$

where i is the event index; k is the weather type index (belonging to the 24 types of extreme weather defined in this study); I_k indicates whether the k-th type of weather occurred (1 = True, 0 = False); $Severity_{i,k}$ is the intensity level of the weather (grades 1–5); $Overlap_{i,k}$ is the proportion of temporal overlap (0–1).

(3) Multi-hazard Exposure (MHE)

The number of distinct extreme weather types experienced in a county-year, reflecting the diversity of compound hazard exposure [64].

$$\text{MHE} = |\{Type_k | k \in \text{extreme weather events}\}|$$

where $|\cdot|$ denotes the cardinality of the set, i.e., the count of unique elements; $Type_k$ denotes the type of the k-th weather event.

(4) Seasonal Concentration (SC)

The degree of unevenness in the seasonal distribution of outage events measured using the Gini coefficient, reflecting the seasonal clustering characteristics of outages [65].

$$\text{SC} = \frac{\sum_i \sum_j |x_i - x_j|}{2n^2 \times \mu}$$

where x_i, x_j are the numbers of outage events in the i-th and j-th quarters, respectively; $n = 4$ (number of quarters); μ is the average number of events per quarter. This indicator ranges from $[0,\ 1]$.

(5) Weather Warning Coverage (WWC)

The proportion of outage events for which meteorological warnings were issued in advance, reflecting the effectiveness and foresight of the warning system [66].

$$\text{WWC} = \frac{N_{warned}}{N_{total}} \times 100\%$$

where N_{warned} is the number of events for which an NWS warning was issued within 24 h prior to the event occurrence.

3. Internal system complexity (ISC)

(1) Renewable Penetration Rate (RPR)

The proportion of installed wind and solar renewable energy capacity to the total installed capacity, reflecting the degree of renewable integration in the energy mix [8].

$$\text{RPR} = \frac{Cap_{wind} + Cap_{solar}}{Cap_{total}} \times 100\%$$

where Cap_{wind} is the installed wind power capacity (MW); Cap_{solar} is the installed photovoltaic capacity (MW); Cap_{total} is the total installed capacity (MW).

(2) Generation Volatility (GV)

The coefficient of variation of monthly renewable energy generation, reflecting the stability and seasonal fluctuation of power supply [8].

$$\text{GV} = \frac{\sigma_{gen}}{\mu_{gen}}$$

where σ_{gen} is the standard deviation of monthly generation over 12 months (MWh); μ_{gen} is the mean of monthly generation over 12 months (MWh).

(3) Infrastructure Aging Index (IAI)

The weighted average operational age of power generation facilities, reflecting the aging degree of grid infrastructure [67].

$$\text{IAI} = \frac{\sum_{i=0}^{n}(Age_i \times Cap_i)}{\sum_{i=0}^{n}(Cap_i)}$$

where Age_i is the operational age (in years) of the i-th generating unit; Cap_i is the installed capacity (MW) of the i-th generating unit. The operational age is calculated as the current year minus the commissioning year.

(4) Peak-hour Outage Ratio (PHOR)

The proportion of outage events occurring during peak electricity demand periods, reflecting system vulnerability under high-load conditions [68].

$$\text{POR} = \left(\frac{N_{peak}}{N_{total}}\right) \times 100\%$$

where N_{peak} is the number of outage events whose start time falls within peak hours (7:00–9:00 and 17:00–21:00 on weekdays).

(5) Distribution Automation Rate (DAR)

The proportion of customers equipped with smart meters, reflecting the modernization and intelligence level of the distribution network [47].

$$\text{DAR} = \frac{N_{smart}}{N_{total}} \times 100\%$$

where N_{smart} is the number of customers with smart meters installed.

(6) Demand Response Capability (DCI)

The ratio of the actual peak load reduction capacity achieved through demand-side management to its potential under emergency conditions [69].

$$\mathrm{DRC} = \frac{Actual_{peak}}{Potential_{peak}}$$

where $Actual_{peak}$ is the actual peak shaving capacity achieved in the county (MW); $Potential_{peak}$ is the potential peak shaving capacity in the county (MW). This indicator ranges from [0, 1]. A DRC = 1 indicates fully realized demand response capability (actual reduction meets potential), while DRC = 0 indicates no realization (no actual reduction or no potential).

(7) Number of Power Supply Units (NPSU)

The number of distribution entities providing electricity service within a county, reflecting the diversity of service providers and the complexity of the management structure [47].

$$\mathrm{NPSU} = Count(\text{Power Supply Units})$$

where "Power Supply Units" refer to the distribution service providers supplying electricity to the county. The indicator value is obtained by counting their number.

4. Social impact complexity (SIC)

(1) Cumulative Outage Exposure Burden (COEB)

The cumulative customer-outage time burden within a county-year unit, standardized as per capita annual outage exposure hours [16].

$$\mathrm{COBE} = \frac{\sum_{event} C_{out,event} \times \Delta t_{event}}{C_{total} \times 8760} \times 1000$$

where $C_{out,event}$ is the number of customers affected by the outage event; C_{total} is the total number of customers in the county for that year; Δt_{event} is the duration of the event (hours); 8760 is the total number of hours in a year.

(2) Population Density Weighted Exposure (PDWE) [70]

$$\mathrm{PDWE} = max\left(PDWE_{day}, PDWE_{night}\right)$$

$$\mathrm{PDWE}_{day} = \frac{E_{day,pop}}{AREA_{SQMI}} \times AOR_{day,time} \times (1 + RPL\_THEMES)$$

$$\mathrm{PDWE}_{night} = \frac{E_{tot,pop}}{AREA_{SQMI}} \times AOR_{night,time} \times (1 + RPL\_THEMES)$$

where $E_{day,pop}$ is the daytime population; $E_{tot,pop}$ is the total resident population; $AREA_{SQMI}$ is the county area (square miles); $AOR_{day,time}$ and $AOR_{night,time}$ are the average outage rates for events occurring during daytime and nighttime, respectively; RPL_THEMES is the overall social vulnerability ranking from the CDC SVI (reflecting "under the same density, higher SVI areas pose higher risk").

(3) Social Vulnerability Exposure Intensity (SVEI)

Integrates the nonlinear relationship between the Social Vulnerability Index and outage impact, reflecting the comprehensive exposure risk of vulnerable populations to power outages [71].

$$\text{SVEI} = RPL\_THEMES \times \Gamma(\text{AOR})$$

where $\Gamma(x) = 1 - e^{-kx}$ representing the exposure impact factor for outage effects, with the nonlinear function capturing threshold effects. In this study, $k = 2$.

(4) Economic Activity Disruption Intensity (EADI)

Estimates the potential economic output loss intensity per capita based on income and outage parameters [72].

$$\text{EADI} = E\_PCI \times \text{AOR} \times \text{AD} \times (1 + EP\_POV)$$

where E_PCI (Per Capita Income Estimate) is the estimated per capita income ($/person); AD is the average outage duration (hours) for the county; EP_POV (Percentage of Persons Below Poverty Estimate) is the estimated poverty rate for the county.

Appendix B

Table A1. Comparison of Core Performance Metrics Across Machine Learning Models.

Model	F1 Score	Accuracy	Precision	Recall	AUC-ROC
XGBoost (this study)	0.9539	0.9539	0.9524	0.9554	0.9933
AdaBoost	0.9502	0.9507	0.9579	0.9427	0.9919
Random Forest (RF)	0.9459	0.9459	0.9459	0.9459	0.9919
Support Vector Machine (SVM)	0.9148	0.9141	0.9062	0.9236	0.9753
Logistic Regression (LR, baseline)	0.8234	0.8317	0.8276	0.8192	0.8912

Appendix C

Supplementary Tables of Core Indicators under Multi-Threshold Schemes.

Note: This appendix provides additional details of the label-threshold robustness analysis that are not fully presented in the main text. All analyses maintain the same model structure, hyperparameters, training logic, and data specifications as the baseline (median) scheme to ensure the unbiased nature of the validation results.

Table A2. Complete Model Classification Performance under Different Threshold Schemes.

Performance Metric	50/50 Baseline Scheme	40/60 Scheme	60/40 Scheme
Accuracy	0.9539	0.9523	0.9316
Precision	0.9524	0.9554	0.9231
Recall	0.9554	0.9655	0.9048
F1 Score	0.9539	0.9604	0.9138
AUC-ROC	0.9933	0.9910	0.9813

Table A3. Complete Comparison of Top 10 Feature Rankings under Different Threshold Schemes.

Rank	50/50 Scheme	40/60 Scheme	60/40 Scheme
1	COEB	COEB	COEB
2	Events	Events	Events
3	LER	LER	LER
4	SVEI	AOR	AOR
5	AOR	SVEI	EADI

Table A3. *Cont.*

Rank	50/50 Scheme	40/60 Scheme	60/40 Scheme
6	EADI	EADI	LDER
7	LDER	DCI	RR
8	WWC	LDER	WOC
9	SC	RR	MSI
10	DCI	MSI	NPSU

The same color indicates the metrics that appear identically across the three threshold schemes.

Appendix D

Table A4. Comparison of Core Model Performance with and Without Resampling.

Performance Metric	With SMOTE + Tomek Links	Without Resampling	Change
F1 Score	0.9539	0.9487	+0.52%
Accuracy	0.9539	0.9493	+0.46%
Precision	0.9524	0.9448	+0.76%
Recall	0.9554	0.9526	+0.28%
AUC-ROC	0.9933	0.9918	+0.15%

Appendix E

Table A5. Optimized Hyperparameters of the XGBoost Model.

Hyperparameter	Search Range	Final Value	Description
n_estimators	[100, 200, 300, 400, 500]	500	Number of weak learners (trees)
max_depth	[3, 5, 7, 9, 11]	7	Maximum tree depth (controls model complexity)
learning_rate	[0.01, 0.05, 0.1, 0.2]	0.05	Learning rate (step size shrinkage)
subsample	[0.6, 0.7, 0.8, 0.9, 1.0]	0.9	Sample ratio per tree
colsample_bytree	[0.6, 0.7, 0.8, 0.9, 1.0]	0.7	Feature sampling ratio per tree
min_child_weight	[1, 3, 5, 7]	1	Minimum sum of instance weight in a child node
gamma	[0, 0.1, 0.2, 0.3]	0.1	Minimum loss reduction required for a split
reg_alpha	[0, 0.1, 1, 10]	0.1	L1 regularization coefficient
reg_lambda	[1, 1.5, 2, 3]	1.5	L2 regularization coefficient

References

1. Ghanbari, M.; Jiang, J. A comprehensive review on power system resilience: Definition, assessment, and enhancement strategies. *Int. J. Electr. Power Energy Syst.* **2025**, *172*, 111149. [CrossRef]
2. Souto, L.; Yip, J.; Wu, W.-Y.; Austgen, B.; Kutanoglu, E.; Hasenbein, J.; Yang, Z.-L.; King, C.W.; Santoso, S. Power system resilience to floods: Modeling, impact assessment, and mid-term mitigation strategies. *Int. J. Electr. Power Energy Syst.* **2022**, *135*, 107545. [CrossRef]

3. Xu, L.; Feng, K.; Lin, N.; Perera, A.; Poor, H.V.; Xie, L.; Ji, C.; Sun, X.A.; Guo, Q.; O'mAlley, M. Resilience of renewable power systems under climate risks. *Nat. Rev. Electr. Eng.* **2024**, *1*, 53–66. [CrossRef]
4. Aghdam, F.H.; Zavodovski, A.; Adetunji, A.; Rasti, M.; Pongracz, E.; Javadi, M.S.; Catalão, J.P. Co-optimization of demand response aggregators and distribution system operator for resilient operation using machine learning-based wind generation forecasting: A bilevel approach. *Int. J. Electr. Power Energy Syst.* **2025**, *164*, 110399. [CrossRef]
5. Bie, Z.; Lin, Y.; Li, G.; Li, F. Battling the extreme: A study on the power system resilience. *Proc. IEEE* **2017**, *105*, 1253–1266. [CrossRef]
6. Yu, Y.; Yan, J.; Wang, Y.; Wang, T.; Zhang, S. Enabling forecasting-aided state estimation in active distribution networks via GLKAN-GRformer-driven pseudo-measurement modeling. *IEEE Trans. Ind. Appl.* **2025**. [CrossRef]
7. Arif, A.; Wang, Z.; Wang, J.; Chen, C. Power distribution system outage management with co-optimization of repairs, reconfiguration, and DG dispatch. *IEEE Trans. Smart Grid* **2018**, *9*, 4109–4118. [CrossRef]
8. Xu, L.; Lin, N.; Poor, H.V.; Xi, D.; Perera, A.T.D. Quantifying cascading power outages during climate extremes considering renewable energy integration. *Nat. Commun.* **2025**, *16*, 2582. [CrossRef]
9. Ganz, S.C.; Duan, C.; Ji, C. Socioeconomic vulnerability and differential impact of severe weather-induced power outages. *PNAS Nexus* **2023**, *2*, pgad295. [CrossRef]
10. Flores, N.M.; McBrien, H.; Do, V.; Kiang, M.V.; Schlegelmilch, J.; Casey, J.A. The 2021 Texas power crisis: Distribution, duration, and disparities. *J. Expo. Sci. Environ. Epidemiol.* **2023**, *33*, 21–31. [CrossRef]
11. UT Austin. Events: February 2021 Texas Blackout. Available online: https://energy.utexas.edu/sites/default/files/UTAustin%20(2021)%20EventsFebruary2021TexasBlackout%2020210714.pdf (accessed on 24 December 2025).
12. Xu, L.; Lin, N.; Xi, D.; Feng, K.; Poor, H.V. Hazard resistance-based spatiotemporal risk analysis for distribution network outages during hurricanes. *IEEE Trans. Power Syst.* **2025**, *40*, 2143–2152. [CrossRef]
13. Feng, K.; Lin, N.; Gori, A.; Xi, D.; Ouyang, M.; Oppenheimer, M. Hurricane Ida's blackout-heatwave compound risk in a changing climate. *Nat. Commun.* **2025**, *16*, 4533. [CrossRef]
14. Boretti, A. Investigating the correlation between extreme temperature events and the increasing frequency of power outages in the Northern Territory of Australia. *Int. J. Electr. Power Energy Syst.* **2024**, *155*, 109608. [CrossRef]
15. Flores, N.M.; Northrop, A.J.; Do, V.; Gordon, M.; Jiang, Y.; Rudolph, K.E.; Hernández, D.; Casey, J.A. Powerless in the storm: Severe weather-driven power outages in New York State, 2017–2020. *PLoS Clim.* **2024**, *3*, e0000364. [CrossRef]
16. Do, V.; McBrien, H.; Flores, N.M.; Northrop, A.J.; Schlegelmilch, J.; Kiang, M.V.; Casey, J.A. Spatiotemporal distribution of power outages with climate events and social vulnerability in the USA. *Nat. Commun.* **2023**, *14*, 2470. [CrossRef]
17. Ma, J.; Li, B.; Omitaomu, O.A.; Mostafavi, A. Establishing nationwide power system vulnerability index across US counties using interpretable machine learning. *Appl. Energy* **2025**, *397*, 126360. [CrossRef]
18. Zhou, R.Z.; Hu, Y.; Zou, L.; Cai, H.; Zhou, B. Understanding the disparate impacts of the 2021 Texas winter storm and power outages through mobile phone location data and nighttime light images. *Int. J. Disaster Risk Reduct.* **2024**, *103*, 104339. [CrossRef]
19. Dugan, J.; Mohagheghi, S. Social vulnerability to long-duration power outages: A survey of households in Colorado and Minnesota. *Electr. J.* **2025**, *38*, 107506. [CrossRef]
20. Loni, A.; Asadi, S. A data-driven approach to quantify social vulnerability to power outages: California case study. *Appl. Energy* **2024**, *359*, 122739. [CrossRef]
21. Rouhana, F.; Zhu, J.; Bagtzoglou, A.C.; Burton, C.G. Analyzing structural inequalities in natural hazard-induced power outages: A spatial-statistical approach. *Int. J. Disaster Risk Reduct.* **2025**, *117*, 105184. [CrossRef]
22. Marcotullio, P.J.; Braçe, O.; Lane, K.; Olson, C.E.; Tipaldo, J.; Ventrella, J.; Yoon, L.; Knowlton, K.; Anand, G.; Matte, T. Local power outages, heat, and community characteristics in New York City. *Sustain. Cities Soc.* **2023**, *99*, 104932. [CrossRef]
23. Najafi-Shad, S.; Mollashahi, M.; Sadr, S.M. A new evaluation method for customer outage costs using long-term outage data and Monte Carlo simulation. *Int. J. Electr. Power Energy Syst.* **2024**, *159*, 110061. [CrossRef]
24. Hou, H.; Zhu, S.; Geng, H.; Li, M.; Xie, Y.; Zhu, L.; Huang, Y. Spatial distribution assessment of power outage under typhoon disasters. *Int. J. Electr. Power Energy Syst.* **2021**, *132*, 107169. [CrossRef]
25. Prieto-Godino, L.; Peláez-Rodríguez, C.; Pérez-Aracil, J.; Pastor-Soriano, J.; Salcedo-Sanz, S. Predicting weather-related power outages in large-scale distribution grids with deep learning ensembles. *Int. J. Electr. Power Energy Syst.* **2025**, *170*, 110811. [CrossRef]
26. Rastgoo, R.; Amjady, N.; Islam, S.; Kamwa, I.; Muyeen, S.M. Extreme outage prediction in power systems using a new deep generative Informer model. *Int. J. Electr. Power Energy Syst.* **2025**, *167*, 110627. [CrossRef]
27. Arora, P.; Ceferino, L. Probabilistic and machine learning methods for uncertainty quantification in power outage prediction due to extreme events. *Nat. Hazards Earth Syst. Sci.* **2023**, *23*, 1665–1683. [CrossRef]
28. Donaldson, L. *The Contingency Theory of Organizations*; Sage Publications: New York, NY, USA, 2001. [CrossRef]
29. Luthans, F.; Stewart, T.I. A general contingency theory of management. *Acad. Manag. Rev.* **1977**, *2*, 181–195. [CrossRef]

30. Nguyen, T.L. Contingency theory in management accounting: A systematic literature review. *Int. J. Adv. Multidiscip. Res. Stud.* **2024**, *4*, 1160–1164.
31. Al-Mahrouqi, M.; Shafieezadeh, A.; Hur, J.; Jung, J.-W.; Ha, J.-G.; Hahm, D. Data-driven predictive models for wind-induced transmission line interruptions. *Int. J. Electr. Power Energy Syst.* **2025**, *171*, 110969. [CrossRef]
32. Yarveysi, F.; Alipour, A.; Moftakhari, H.; Jafarzadegan, K.; Moradkhani, H. Block-level vulnerability assessment reveals disproportionate impacts of natural hazards across the conterminous United States. *Nat. Commun.* **2023**, *14*, 4222. [CrossRef] [PubMed]
33. *IEEE Std 1366-2022*; IEEE Guide for Electric Power Distribution Reliability Indices. IEEE Standards Association: New York, NY, USA, 2022. Available online: https://standards.ieee.org/ieee/1366/7243/ (accessed on 24 December 2025).
34. Belsley, D.A.; Kuh, E.; Welsch, R.E. *Regression Diagnostics: Identifying Influential Data and Sources of Collinearity*; John Wiley & Sons: New York, NY, USA, 1980. [CrossRef]
35. Rodríguez-Avellaneda, A.H.; Rodriguez, R.; Shafieezadeh, A.; Yilmaz, A. Socioeconomic disparities in hurricane-induced power outages: Insights from multi-hurricane data in Florida using XGBoost. *Sustain. Cities Soc.* **2025**, *126*, 106362. [CrossRef]
36. Zhang, Y.; Su, H.; Wang, R.; Deng, J.; Wang, Y.; Guo, W.; Li, R. Short-term forecast method of wind power output based on multi-scale CNN–LSTM in extreme weather. *Int. J. Electr. Power Energy Syst.* **2025**, *172*, 111191. [CrossRef]
37. Liu, H.; Lu, J.; Li, X.; Wang, Y.; Xu, D.; Yin, J.; Xu, G. Evaluating human–nature relationships at a grid scale in China, 2000–2020. *Habitat Int.* **2025**, *156*, 103282. [CrossRef]
38. Gedamu, W.T.; Plank-Wiedenbeck, U.; Wodajo, B.T. A spatial autocorrelation analysis of road traffic crash by severity using Moran's I spatial statistics: A comparative study of Addis Ababa and Berlin cities. *Accid. Anal. Prev.* **2024**, *200*, 107535. [CrossRef]
39. Figshare. The Environment for Analysis of Geo-Located Energy Information's Recorded Electricity Outages 2014–2024 (Dataset). Available online: https://figshare.com/articles/dataset/The_Environment_for_Analysis_of_Geo-Located_Energy_Information_s_Recorded_Electricity_Outages_2014-2022/24237376 (accessed on 24 December 2025).
40. U.S. Census Bureau. TIGER/Line Shapefiles. Available online: https://www.census.gov/geographies/mapping-files/time-series/geo/tiger-line-file.html (accessed on 24 December 2025).
41. U.S. Census Bureau. County Adjacency File. 2023. Available online: https://www.census.gov/geographies/reference-files/2023/geo/county-adjacency.html (accessed on 24 December 2025).
42. U.S. Energy Information Administration (EIA). Electricity Market Module of the National Energy Modeling System: Model Documentation (AEO2025). Available online: https://www.eia.gov/outlooks/aeo/nems/documentation/electricity/pdf/EMM_AEO2025.pdf (accessed on 24 December 2025).
43. NOAA NCEI. Storm Events Database. Available online: https://www.ncei.noaa.gov/stormevents/ftp.jsp (accessed on 24 December 2025).
44. Iowa Environmental Mesonet (IEM). NWS Watches Warnings Advisories Download. Available online: https://mesonet.agron.iastate.edu/request/gis/watchwarn.phtml (accessed on 24 December 2025).
45. ATSDR. SVI Data & Documentation Download (GRASP). Available online: https://www.atsdr.cdc.gov/place-health/php/svi/svi-data-documentation-download.html (accessed on 24 December 2025).
46. U.S. Energy Information Administration (EIA). Form EIA-860 Detailed Data. Available online: https://www.eia.gov/electricity/data/eia860/ (accessed on 24 December 2025).
47. U.S. Energy Information Administration (EIA). Form EIA-861 Detailed Data Files. Available online: https://www.eia.gov/electricity/data/eia861/ (accessed on 24 December 2025).
48. U.S. Energy Information Administration (EIA). Form EIA-923 Detailed Data. Available online: https://www.eia.gov/electricity/data/eia923/ (accessed on 24 December 2025).
49. Dobson, I.; Carreras, B.A.; Lynch, V.E.; Newman, D.E. Complex systems analysis of series of blackouts: Cascading failure, critical points, and self-organization. *Chaos* **2007**, *17*, 026103. [CrossRef]
50. Hartmann, B.; Deng, S.; Ódor, G.; Kelling, J. Visiting and modeling power-law distributions in empirical outage data of power. *PRX Energy* **2023**, *2*, 033007. [CrossRef]
51. Augurisk. Tensas Parish, Louisiana Natural Disaster Risk Assessment. Available online: https://www.augurisk.com/risk/state/louisiana/tensas-parish/22107 (accessed on 24 December 2025).
52. Louisiana United Way. ALICE Report County Snapshots (LA): Tensas County. Available online: https://www.launitedway.org/sites/launitedway/files/ALICE%202025/Tensas.pdf (accessed on 24 December 2025).
53. Durham County. Climate Resilience. Available online: https://zh-cn.dconc.gov/Engineering-and-Environmental-Services/Sustainability/Climate-Resilience (accessed on 24 December 2025).
54. U.S. Climate Vulnerability Index. Socioeconomic Stressors in Henderson County, NC. Available online: https://map.climatevulnerabilityindex.org/report/social_economic_socioeconomic_stressors/henderson-county-north-carolina (accessed on 24 December 2025).

55. ArcGIS StoryMaps. Flood Risk in New Hanover County and Adjacent Areas. Available online: https://storymaps.arcgis.com/stories/d7e30e4f043f414c90ddda85c5dfb55c (accessed on 24 December 2025).
56. Ulak, M.B.; Kocatepe, A.; Sriram, L.M.K.; Ozguven, E.E.; Arghandeh, R. Assessment of the hurricane-induced power outages from a demographic, socioeconomic, and transportation perspective. *Nat. Hazards* **2018**, *92*, 1489–1508. [CrossRef]
57. Stødle, K.; Flage, R.; Guikema, S.D. Identifying power outage hotspots to support risk management planning. *Risk Anal.* **2025**, *45*, 1271–1281. [CrossRef] [PubMed]
58. Al-Shaalan, A.M. Reliability Evaluation of Power Systems. In *Reliability and Maintenance—An Overview of Cases*; IntechOpen: London, UK, 2020. [CrossRef]
59. Nateghi, R.; Guikema, S.D.; Quiring, S.M. Comparison and validation of statistical methods for predicting power outage durations in the event of hurricanes. *Risk Anal.* **2011**, *31*, 1897–1906. [CrossRef]
60. Everitt, B.S.; Skrondal, A. *The Cambridge Dictionary of Statistics*, 4th ed.; Cambridge University Press: Cambridge, UK, 2010; p. 98.
61. Kezunovic, M.; Xie, L.; Grijalva, S. The role of big data in improving power system operation and protection. In Proceedings of the 2013 IREP Symposium Bulk Power System Dynamics and Control—IX Optimization, Security and Control of the Emerging Power Grid, Rethymno, Greece, 25–30 August 2013; pp. 1–9. [CrossRef]
62. Campbell, R.J. *Weather-Related Power Outages and Electric System Resiliency*; Congressional Research Service Report for Congress: Washington, DC, USA, 2012; pp. 4–6.
63. Panteli, M.; Mancarella, P. Influence of extreme weather and climate change on the resilience of power systems: Impacts and possible mitigation strategies. *Electr. Power Syst. Res.* **2015**, *127*, 259–270. [CrossRef]
64. Gill, J.C.; Malamud, B.D. Reviewing and visualizing the interactions of natural hazards. *Rev. Geophys.* **2014**, *52*, 680–722. [CrossRef]
65. Glasser, G.J. Variance formulas for the mean difference and coefficient of concentration. *J. Am. Stat. Assoc.* **1962**, *57*, 648–654. [CrossRef]
66. Cao, Z.; Feng, Y.; Li, X. A study on the calculation method for the coverage rate of early warning release. *IOP Conf. Ser. Earth Environ. Sci.* **2019**, *233*, 052034. [CrossRef]
67. Eto, J.H.; LaCommare, K.H. *Tracking the Reliability of the U.S. Electric Power System: An Assessment of Publicly Available Information Reported to State Public Utility Commissions*; Lawrence Berkeley National Laboratory Report LBNL-1092E; LBNL: Berkeley, CA, USA, 2008; pp. 34–36.
68. Hines, P.; Apt, J.; Talukdar, S. Large blackouts in North America: Historical trends and policy implications. *Energy Policy* **2009**, *37*, 5249–5259. [CrossRef]
69. Cappers, P.; Goldman, C.; Kathan, D. Demand response in U.S. electricity markets: Empirical evidence. *Energy* **2010**, *35*, 1526–1535. [CrossRef]
70. Cutter, S.L.; Boruff, B.J.; Shirley, W.L. Social vulnerability to environmental hazards. *Soc. Sci. Q.* **2003**, *84*, 242–261. [CrossRef]
71. Flanagan, B.E.; Gregory, E.W.; Hallisey, E.J.; Heitgerd, J.L.; Lewis, B. A social vulnerability index for disaster management. *J. Homel. Secur. Emerg. Manag.* **2011**, *8*, 1792. [CrossRef]
72. Rose, A.; Liao, S.Y. Modeling regional economic resilience to disasters: A computable general equilibrium analysis of water service disruptions. *J. Reg. Sci.* **2005**, *45*, 75–112. [CrossRef]

Disclaimer/Publisher's Note: The statements, opinions and data contained in all publications are solely those of the individual author(s) and contributor(s) and not of MDPI and/or the editor(s). MDPI and/or the editor(s) disclaim responsibility for any injury to people or property resulting from any ideas, methods, instructions or products referred to in the content.